Perfluoropolyalkylether Maleimides for Protection From Oxygen Inhibition and Surface Modification of Photoinitiator-Free UV-Cured Polymers

frontiers in Materials

ORIGINAL RESEARCH
published: 23 January 2020
doi: 10.3389/fmats.2019.00346

Perfluoropolyalkylether Maleimides for Protection From Oxygen Inhibition and Surface Modification of Photoinitiator-Free UV-Cured Polymers

*Céline Bonneaud[1], Julia Burgess[2], Alessandra Vitale[3], Giuseppe Trusiano[3], Christine Joly-Duhamel[1], Chadron M. Friesen[2] and Roberta Bongiovanni[3]**

[1] Ingénierie et Architectures Macromoléculaires, Institut Charles Gerhardt, Univ Montpellier, Ecole Nationale Supérieure de Montpellier (UMR5253-CNRS), Montpellier, France, [2] Department of Chemistry, Trinity Western University, Langley, BC, Canada, [3] Department of Applied Science & Technology, Politecnico di Torino, Turin, Italy

OPEN ACCESS

Edited by:
Wenbo Wang,
Lanzhou Institute of Chemical Physics (CAS), China

Reviewed by:
Tom Scherzer,
Leibniz Institute of Surface Modification (LG), Germany
Allan Guymon,
The University of Iowa, United States

***Correspondence:**
Roberta Bongiovanni
roberta.bongiovanni@polito.it

Specialty section:
This article was submitted to Polymeric and Composite Materials, a section of the journal Frontiers in Materials

Received: *21 August 2019*
Accepted: *27 December 2019*
Published: *23 January 2020*

Citation:
Bonneaud C, Burgess J, Vitale A, Trusiano G, Joly-Duhamel C, Friesen CM and Bongiovanni R (2020) Perfluoropolyalkylether Maleimides for Protection From Oxygen Inhibition and Surface Modification of Photoinitiator-Free UV-Cured Polymers. Front. Mater. 6:346. doi: 10.3389/fmats.2019.00346

Maleimides are attractive systems for photopolymerize for two major reasons: (1) they follow a radical mechanism without requiring a photoinitiator and (2) their rate of polymerization corresponds similarly to acrylates, which are commonplace in the industry. In this work, bismaleimide polypropylene oxide was cured under UV light forming thin films. Their surface properties were modified by copolymerization them with fluorinated comonomers. To this goal, perfluoropolyalkylethers (PFPAEs) with maleimide groups were synthesized, varying their chain structure, their functionality degree and consequently their intrinsic viscosity. These PFPPAE comonomers were highlighted to segregate at the surface, assuring omniphobic properties and acting as a protective layer against oxygen inhibition. These phenomenon were observed even when added at a concentration $\leq$5% w/w with respect to the main polypropylene oxide monomer. XPS analyses confirmed the segregation of the fluorine atoms at the surface during the UV-curing process of the coatings.

Keywords: UV-curing, maleimides, fluoropolymer, perfluoropolyalkylether, surface properties

INTRODUCTION

Photoinduced polymerizations are green processes suitable for the sustainable synthesis of polymers (Bowman and Kloxin, 2008; Yagci et al., 2010; Corrigan et al., 2019). In fact, they are bulk processes (without solvent) which require low amount of energy as they occur at room temperature. Indeed these photoinduced reactions are very fast: the reaction time for achieving quantitative conversion is of the order of seconds or minutes. Most photoinduced polymerizations are chain reactions, initiated by a proper photoinitiator able to absorb light, reach an excited state and originate reactive species; if the functionality of the monomers is $\geq$2, cross-linked networks are formed. Thus, from a liquid resin, a solid material can be easily obtained after a few seconds of light irradiation. Currently, UV and LED sources are used for these methods but the amount of curing depends on the absorbance of light, thus monomers are preferably

processed in the form of thin films. Consequently, since the start of its industrial development, UV-curing finds application in fields such as paints, adhesives or protective coatings. At the present time, cutting-edge technologies such as 3D-printing and medical implants benefit from these processes: in fact they can be controlled in time and space as the monomers react only in the irradiated area and the polymerization stops when the light is switched off (Ligon et al., 2017). Commonly, monomers employed in the photoinduced processes used for the above applications, are acrylic, methacrylic and thiol-ene systems (Hoyle and Bowman, 2010; Crivello and Reichmanis, 2014; Du et al., 2017a,b). Maleimides represent an attractive alternative as they polymerize almost as fast as acrylates. Their photopolymerization in bulk and in solution was reported for the first time by Yamada et al. (1968); the mechanism of initiation was found to be based on an electron transfer able to provide a radical anion (von Sonntag et al., 1999; von Sonntag and Knolle, 2000). In the last decade, homopolymerization under UV-light of maleimides containing different backbones such as ethylene glycol (Vázquez et al., 2009), perfluoroalkyl chains (Soules et al., 2008), or siloxanes (Pozos vázquez et al., 2010) was explored. Results confirmed that the reaction is very efficient even in the absence of a photoinitiator (Decker et al., 2004; Vázquez et al., 2009). This is of major relevance in fields where photopolymers are applied, as the presence of photoinitiators often poses safety issues due to their potential leaching. For this reason, maleimides are also proposed as photoinitiators for different types of unsaturated resins such as acrylates, vinyl ethers, etc. (Hoyle et al., 1997; Jönsson et al., 1997).

As previously mentioned, polymers obtained by photopolymerization often come in the form of film and are used as coatings, adhesives, inks where performance depends most importantly on surface properties (i.e., adhesion, wettability, self-cleaning, printability etc.). Tailoring the surface of UV-cured polymers while keeping the bulk properties unchanged is possible by introducing a small amount of a surface-active comonomer in the reactive formulation (Vitale et al., 2018; Wasser et al., 2018). This approach has been widely applied to acrylic, vinyl ether, epoxy systems using fluorinated comonomers (Vitale et al., 2015; Wasser et al., 2018). In this work, we describe the influence of fluorinated maleimides for the modification of photoinitiator-free maleimides-based coatings. In particular, three new fluorinated maleimides were prepared by functionalization of perfluoropolyalkylether chains (PFPAEs) containing one or two of the following repeating units $-(CF_2O)-$, $-(CF_2CF_2O)-$, and $-(CF(CF_3)CF_2O)-$. These highly fluorinated building blocks were chosen as they are both hydro- and oleo-phobic. Moreover, they are known as non-toxic (Ameduri and Boutevin, 2004; Friesen and Ameduri, 2018) with respect to perfluoroalkyl chains (Wang et al., 2015) so that they can be employed in food applications and even in biomedical applications (Malinverno et al., 1996; Pantini, 2008; Zhang et al., 2018). The effect of mono- and bi-functional fluoromaleimides on the photopolymerization of a commercial bismaleimide polypropylene oxide was investigated. Then, their impact on the polymerization kinetics and on the surface properties of the coatings was examined.

MATERIALS AND METHODS

Materials

The commercial bismaleimide poly(propylene oxide) (M_n∼400 g/mol) called BMI PPO was purchased from Specific Polymers (France).

The fluorinated monomaleimide MMI (see structure in **Figure 1**) was synthesized as previously reported (Bonneaud et al., 2019) by esterification of Krytox® Methylene Alcohol, kindly provided by Chemours Company (Wilmington, Delaware, USA).

Two fluorinated bismaleimides, labeled BMI C5 and BMI C10 (see structure in **Figure 1**), were synthesized starting from a commercial perfluoropolyalkylether diol Fluorolink® E10H (M_n∼1,800 g/mol) from Solvay Solexis (Bollate, Italy), purchased from Acota (UK). The reaction was carried out using either 6-maleimidohexanoic acid (to obtain BMI C5) or 11-maleimidoundecanoic acid (to obtain BMI C10). 6-maleimidohexanoic acid, 11-maleimidoundecanoic acid, dicyclohexylcarbodiimide, dimethylamino pyridine, dichloromethane, hexadecane, and chloroform were purchased from Sigma Aldrich (St. Louis, Missouri, USA) and used as received. C_6D_6 was purchased from Eurisotop (Cambridge, UK) and used in capillaries for NMR analyses. 1,1,1,3,3-pentafluorobutane was purchased from Alfa Aesar (Ward Hill, Massachusetts, USA).

Synthesis and Characterization of the Fluorinated Maleimides

The monomaleimide MMI was synthesized following a previous procedure (Bonneaud et al., 2019).

In a typical procedure, to a dichloromethane solution of 6-maleimidohexanoic acid or 11-maleimidoundecanoic acid (2.05 eq), dimethylaminopyridine (0.2 eq) and Fluorolink® E10H (2 eq) in 1,1,1,3,3-pentafluorobutane were added dropwise at 0°C. After 5 min, the ice bath was removed. After 1.5 h, the reaction was stopped. A first filtration was performed and the solvents were partially removed. A liquid-liquid extraction was performed using both 1,1,1,3,3-pentafluorobutane and saturated $NaHCO_3$ (aq). The fluorinated phase was then washed with saturated $NaHCO_3$(aq) (*2) and brine (*1). A second filtration through silica/Celite® was performed. Hydroquinone was added (0.1% w/w) and the solvent was removed.

BMI C5 yield was 73%; BMI C10 yield was 21%. The products were characterized by ^{1}H NMR, ^{13}C NMR, and FT-IR (ATR). NMR spectra were recorded on a Bruker AVANCE III 400 MHz spectrometer instruments using TopSpin 3.5 operating at 400.13 (^{1}H), 376.46 (^{19}F), 100.62 (^{13}C) MHz at room temperature except if specified. C_6D_6 capillaries were used as internal references. The letters s, d, t, q, quint, sext, and spt stand for singlet, doublet, triplet, quartet, quintuplet, sextet, and septuplet, respectively.

BMI C5 ^{1}H NMR (400 MHz, C_6D_6, 25°C):

δ = 1.60 (m, -N(CH_2)$_2$C**H$_2$**(CH_2)$_2$-, 2H), 1.87 (m, -NCH_2C**H$_2$**CH_2C**H$_2$**CH_2C(O)O-, 4H), 2.57 (q, $^3J_{H-H}$ = 7.4 Hz, -CH_2C**H$_2$**C(O)O-, 2H), 3.77 (t, $^3J_{H-H}$ = 7.2 Hz, -NC**H$_2$**-, 2H), 3.93-4.48 (m, -CF_2C**H$_2$**(OC**H$_2$**C**H$_2$**)$_{1.75}$O-, 9H), 6.88 (s, -C(O)C**H**=C**H**C(O)-, 2H)

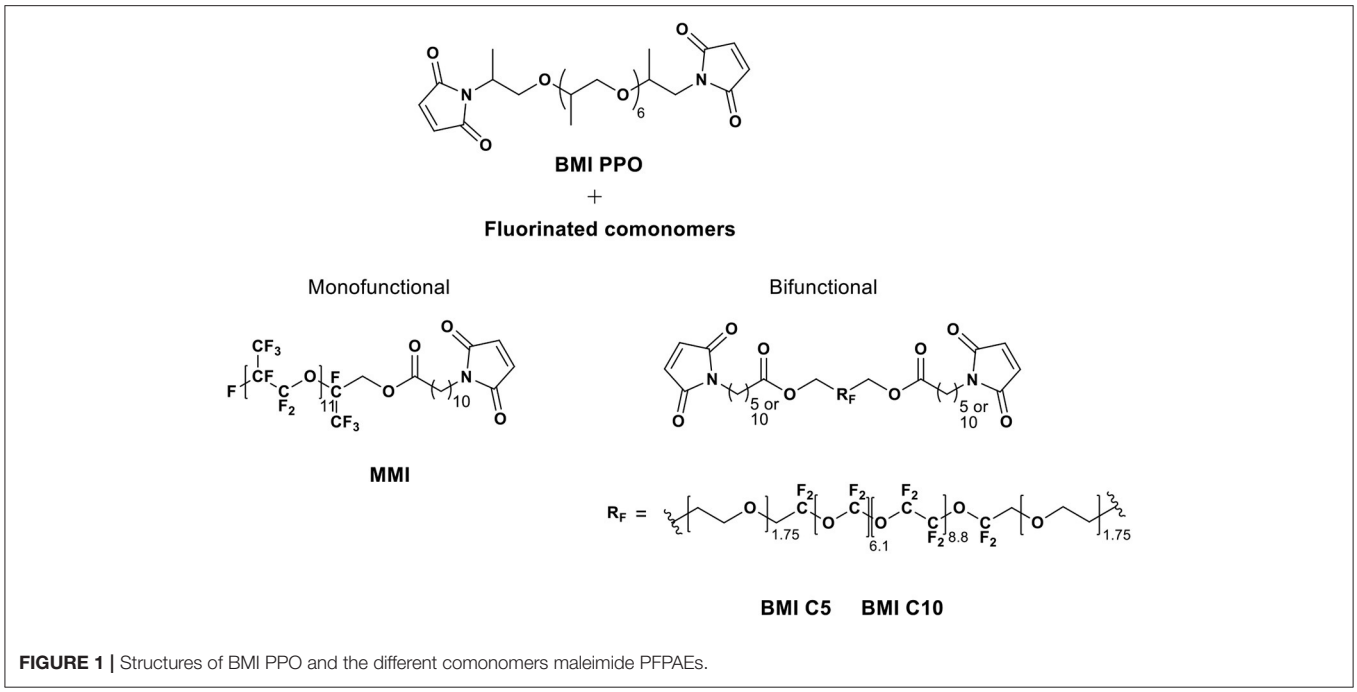

FIGURE 1 | Structures of BMI PPO and the different comonomers maleimide PFPAEs.

BMI C5 ^{13}C NMR (100 MHz, C_6D_6, 25°C):

δ = 24.0 ($N(CH_2)_6\mathbf{C}H_2CH_2C(O)O$-), 26.2 (-$NCH_2CH_2\mathbf{C}H_2$-), 28.3 (-$NCH_2\mathbf{C}H_2$-), 33.7 (-$CH_2\mathbf{C}H_2C(O)O$-), 37.4 (-$N\mathbf{C}H_2$-), 69.2-72.2 (-$CF_2\mathbf{C}H_2(O\mathbf{C}H_2\mathbf{C}H_2)_{1.75}O$-), 134.1 (-$C(O)\mathbf{C}H{=}\mathbf{C}HC(O)$-), 171.1 (-$\mathbf{C}(O)CH{=}CH\mathbf{C}(O)$-), 173.3 (-$CF(CF_3)CH_2O(\mathbf{C}O)$-)

BMI C5 FT-IR (ATR) ν_{max} (cm^{-1}): 695.3 – 828.0 – 1061.4 – 1184.7 – 1706.2 – 2939.5

BMI C10 ^{1}H NMR (400 MHz, C_6D_6, 25°C):

δ = 1.59 (m, -$N(CH_2)_2(C\mathbf{H}_2)_6CH_2$-, 12H), 1.87 (m, -$NCH_2C\mathbf{H}_2(CH_2)_6C\mathbf{H}_2CH_2C(O)O$-, 4H), 2.57 (q, $^3J_{H-H}$ = 7.1 Hz, -$CH_2C\mathbf{H}_2C(O)O$-, 2H), 3.76 (t, $^3J_{H-H}$ = 7.2 Hz, -$NC\mathbf{H}_2$-, 2H), 3.92-4.47 (m, -$CF_2C\mathbf{H}_2(OC\mathbf{H}_2C\mathbf{H}_2)_{1.75}O$-, 9H), 6.87 (br, -$C(O)C\mathbf{H}{=}C\mathbf{H}C(O)$-, 2H)

BMI C10 ^{13}C NMR (100 MHz, C_6D_6, 25°C):

δ = 25.0 ($N(CH_2)_6\mathbf{C}H_2CH_2C(O)O$-), 26.8 (-$NCH_2CH_2\mathbf{C}H_2$-), 28.7 (-$NCH_2\mathbf{C}H_2$-), 29.4-29.6 (-$N(CH_2)_3(\mathbf{C}H_2)_5(CH_2)_2$-), 33.9 (-$CH_2\mathbf{C}H_2C(O)O$-), 37.7 (-$N\mathbf{C}H_2$-), 69.2-72.2 (-$CF_2\mathbf{C}H_2(O\mathbf{C}H_2\mathbf{C}H_2)_{1.75}O$-), 134.1 (-$C(O)\mathbf{C}H{=}\mathbf{C}HC(O)$-), 171.1 (-$\mathbf{C}(O)CH{=}CH\mathbf{C}(O)$-), 173.5 (-$CF(CF_3)CH_2O(\mathbf{C}O)$-)

BMI C10 FT-IR (ATR) ν_{max} (cm^{-1}): 695.3 – 828.4 – 1062.1 – 1185.1 – 1706.8 – 2929.2.

Preparation and Methods of Characterization of the Coatings

Photopolymerization kinetics were monitored by Real-time Infrared Spectroscopy performed on a Thermo Scientific Nicolet 6700 FTIR apparatus using attenuated total reflectance (ATR) methods controlled by OMNIC software. The conversion was monitored by following the disappearance of the vibrational band at 826 cm^{-1} corresponding to the maleimide group; the conversion τ was estimated through the univariate method ($\tau = (1-(A/A_0))*100$). A mercury lamp (OmniCure S2000) was used as UV-light source. An OmniCure R2000 Radiometer was used to control the light output: the intensity at the sample surface was 10 mW/cm². One drop of sample, with no photoinitiator, was deposited on the ATR unit of the infrared spectrometer (thickness ∼ 10–30 μm) for each measurement. A polypropylene film (6 μm) was used as air protector and each experiment was conducted four times.

For the fabrication of films, the reactive monomers (without photoinitiator) were poured onto glass slides previously cleaned with acetones. The coating of the films was done by bar coating (thickness around 25 μm) with a film applicator bar coater (Sheen 1117/100 mm). Irradiation was performed for 5 min with a mercury lamp (Dymax) with an intensity of 150 mW/cm². These films were used for further characterization.

The gel content was determined as $[w_1/w_0] \times 100$, where w_0 is the initial weight of the sample (mg) and w_1 is the weight after extraction (mg). The extraction solvent was chloroform for the BMI PPO-based polymers and 1,1,1,3,3-pentafluorobutane for the fully fluorinated coatings. The films were weighed and then immersed in the extracting solvent for 24 h (three repeats). After the extraction, the films were dried at 45°C under vacuum (10^{-2} mbar) for 24 h and reweighed.

Thermogravimetric analyses (TGA) were carried out with a NETZSCH TG209F1 apparatus, at a heating rate of 20°C min^{-1}. Approximately 10 mg of sample were placed in an alumina crucible and heated from room temperature to 600°C under air (40 mL.min^{-1}).

Differential scanning calorimetry (DSC) was used to determine the glass transition temperatures of the polymers, employing a NETZSCH DSC200F3 calorimeter. Constant

calibration was performed using indium, n-octadecane and n-octane standards. Ten to fifteen mg of sample were placed in an aluminum pan and the thermal properties were recorded between −150 and 100°C at 20°C min^{-1}. Nitrogen was used as the purge gas.

Contact angle measurements were performed by using a contact angle system OCA20 coupled with a CCD-camera from DataPhysics Instrument using the software SCA20 4.1. The measurements were made in air at room temperature by the sessile drop technique 10 s after the deposition of the drop. Distilled water and hexadecane previously dried were the testing liquids. Between three and six repeats were made on three different samples previously irradiated. Their difference in the average value was no more than 3°.

X-ray photoelectron emission spectra were recorded using a monochromatised Al Kalpha ($h\nu = 1486.6$ eV) source on a ThermoScientific K-Alpha system. The X-ray Spot size was about 400 μm. The Pass energy was fixed at 20 eV with a step of 0.1 eV for core levels and 150 eV for surveys (step 1 eV). The spectrometer energy calibration was done using the Au $4f_{7/2}$ (83.9 ± 0.1 eV) and $Ag3d_{5/2}$ (368.2 ± 0.1 eV) photoelectron lines. XPS spectra were recorded in direct mode N (Ec).

The viscosities of BMI C5 and BMI C10 were measured at 25°C on the AR-1000 rheometer (TA Instruments). A 25 mm diameter and 4° cone-plan geometry were used. The flow mode was used with a gradient from 10 to 0.1 s^{-1} and then the steady flow mode from 0.1 to 10 s^{-1}. The viscosity value is the average value over 15 points of the "plateau."

RESULTS AND DISCUSSION

Photocopolymerization of Maleimides

Different maleimides containing a perfluoropolyalkylether chain (PFPAE) and possessing a different functionality were synthesized: the chemical structure of the monomers is reported in **Figure 1**.

The monofunctional fluorinated monomaleimide (MMI) containing hexafluoropropyleneoxide units was synthesized as reported in a previous paper (Bonneaud et al., 2019). Two telechelic difunctional bismaleimides (BMI C5 and BMI C10) were obtained by esterification reaction of maleimidocarboxylic acids of different molecular weight with a commercial fluorinated diol HO-RF-OH, where RF (reported in **Figure 1**) is a fluorinated chain based on –(CF_2O)–, –(CF_2CF_2O)–. Therefore, the fluorinated BMI are characterized by the same perfluoropolyalkylether structure, and have different alkylic spacers –$(CH_2)_n$-, where n =5 or 10 for BMI C5 and BMI C10, respectively.

First, the neat fluorinated maleimides were homopolymerized. As already mentioned, maleimides can initiate the polymerization on their own according to the mechanism of **Figure 2**, where the mechanism of initiation proposed is an electron transfer which provides a radical anion (von Sonntag et al., 1999; von Sonntag and Knolle, 2000).

MMI reaction was studied previously (Bonneaud et al., 2019): it was reported that MMI is a highly reactive monomer with a quantitative conversion observed even in 8 s in the absence of air and in 40 s in the presence of air (see also **Table 1**).

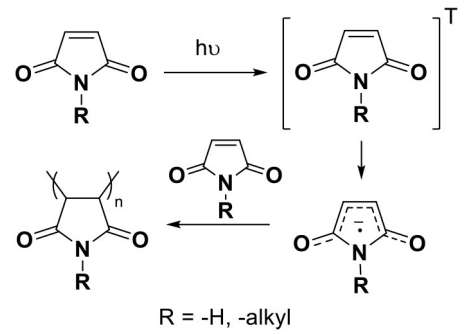

FIGURE 2 | Homopolymerization of monomaleimides by radical mechanism.

TABLE 1 | Conversion of the maleimide in the presence and in the absence of air for different percentages of additives.

Sample	BMI PPO (wt%)	PFPAE additive (wt%)	Conversion after 5 min under air (%)	Conversion after 5 min without air (%)	Gel content (%)
BMI PPO - Neat	100	0	91.9 ± 1.2	96.5 ± 0.1	89 ± 4[a]
BMI PPO + MMI 2%	98	2	96.2 ± 0.3	97.3 ± 0.4	90 ± 4[a]
BMI PPO + MMI 5%	95	5	95.7 ± 0.5	96.8 ± 0.3	95 ± 1[a]
MMI - Neat	0	100	100	100	n/a*
BMI PPO + BMI C5 2%	98	2	n/a	96.5 ± 0.1	94 ± 3[a]
BMI PPO + BMI C5 5%	95	5	95 ± 0.5[c]	96.5 ± 0.2	95 ± 3[a]
BMI C5 - Neat	0	100	n/a	97.5 ± 1.0	95 ± 4[b]
BMI PPO + BMI C10 2%	98	2	95.1 ± 0.3	96.6 ± 0.1	97 ± 2[a]
BMI PPO + BMI C10 5%	95	5	94.8 ± 0.7	96.7 ± 0.1	97 ± 1[a]
BMI C10 - Neat	0	100	n/a	97.5 ± 1.0	95 ± 1[b]

*[a]Measured in chloroform; [b]measured in 1,1,1,3,3-pentafluorobutane; [c]measured at 360 s. *The gel content was not calculated on a linear polymer.*

Having low viscosity, it could be easily coated on glass as a film and under irradiation exhibited high reactivity, giving rise to a linear polymer. As expected, also BMI C5 and BMI C10 were reactive even in the absence of a photoinitiator. The homopolymers obtained from the bifunctional fluorinated maleimides had quantitative conversion as indicated by the high gel content values (**Table 1**). However, the viscosity of BMI C10 was too high and did not allow a uniform coating of substrates, i.e., it is unsuitable for the preparation of coatings through a bulk process.

Therefore, the fluorinated monomers were preferably used in copolymerization with BMI PPO at a low concentration, i.e., 2 w/w% and 5 w/w% resulting in crosslinked polymers in the form of transparent films, 25 μm thick.

The photopolymerization kinetics of the comonomeric mixtures of BMI PPO with each fluoromonomer, were monitored by Real-time Infrared Spectroscopy, by following the

disappearance of the band at 826 cm^{-1} corresponding to the maleimide group. No photoinitiator was added. The irradiation was done both in air and in absence of air: protection from air was obtained covering the monomers with a polypropylene sheet according to common practice. The conversion data vs. time are plotted in **Figure 3**, comparing the reactions with the homopolymerization of BMI PPO.

Neat BMI PPO provided crosslinked films with a high gel content (**Table 1**). On **Figure 3A**, BMI PPO demonstrated that its photopolymerization kinetics was found to be faster combined with a higher yield in the absence of air. In the presence of air, the rate was significantly lower. Indeed, the final conversion never reached the value obtained in the absence of air. Thus, after 5 min of irradiation its value was 91.9% instead of 96.5%.

Figure 3A shows the influence of MMI on the conversion curves. In the absence of air, the addition of MMI slightly slowed down the reaction, the initial rate was lower while the final conversion was higher than the neat BMI PPO, and could be reached at a longer irradiation time. This reduced conversion rate could be ascribed to the lower average functionality of the system as MMI is monofunctional. Being MMI monofunctional, it could however enhance the mobility of the system, thus leading to higher conversion degrees (from 96.5% without MMI to 97.3% with 5 w% of MMI after 5 min of UV irradiation, as shown in **Table 1**). It is worth reporting that the system prior irradiation appeared white and opaque, indicating heterogeneity, while after an exposure of 5 min under UV-light, transparent coatings were formed. Thus heterogeneity was initially present and could have an effect on initial reaction rate: the phase separation may delay the photopolymerization process due to lower light absorption and hindering of reactive species diffusion at/though the interface.

Concerning the copolymerization in the presence of air, the final conversion was always improved by the fluorinated comonomer, as in the case of the reaction performed in the absence of air: from 91.9% without MMI to 96.2% with 5 w% of MMI after 5 min of UV irradiation, as shown in **Table 1**. More interestingly, in the presence of air, the addition of MMI enhanced the speed rate: the higher the percentage of MMI additive, the higher the initial rate. As the photopolymerization kinetics are slower in the presence of air due to the quenching of radicals by oxygen (Ligon et al., 2014), the addition of MMI seems to contrast this inhibition phenomenon. It is known that the fluorinated phase of methacrylate PFPAE with hydrogenated

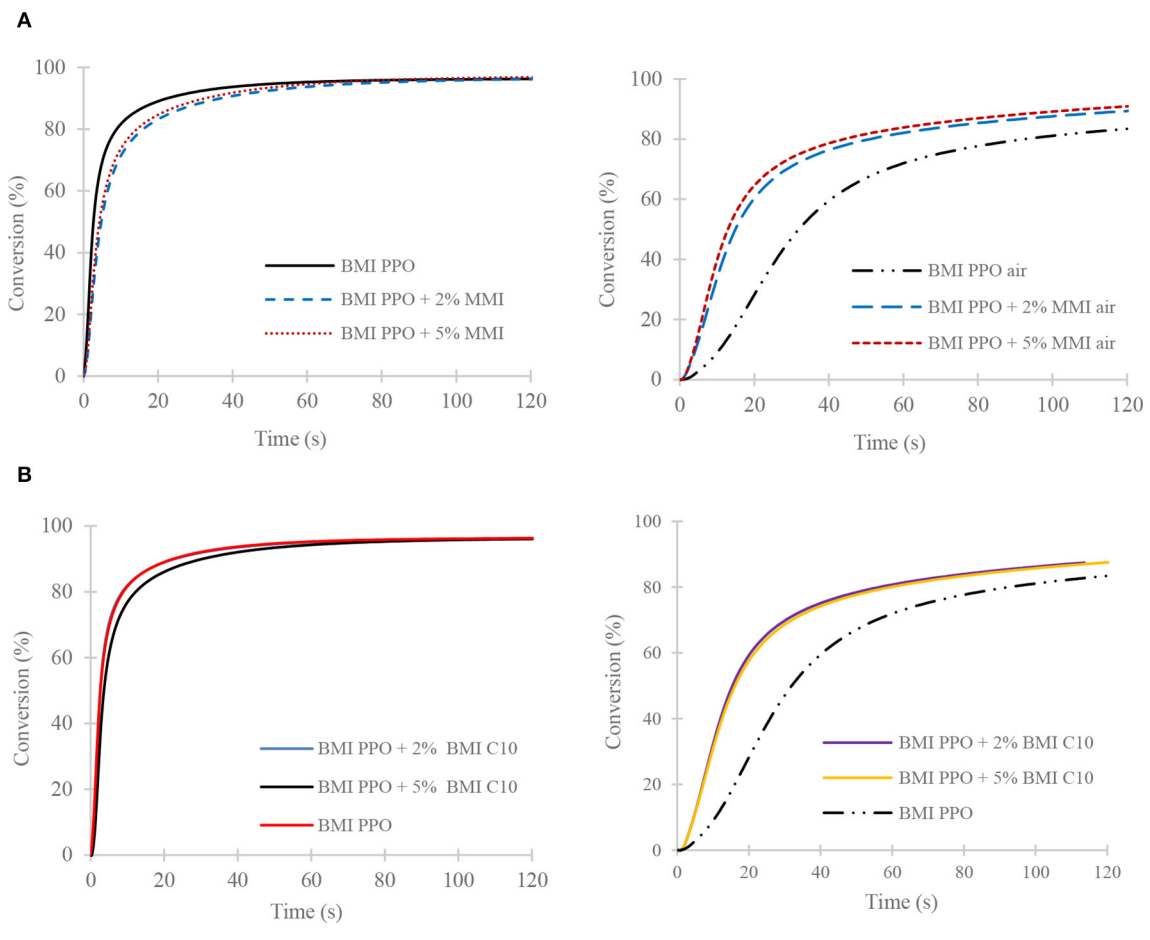

FIGURE 3 | (A) Photopolymerization conversion curves of BMI PPO with different amounts (wt%) of MMI in the absence (left) and presence (right) of air. **(B)** Photopolymerization conversion curves of BMI PPO with different amounts (wt%) of BMI C10 in the absence (left) and presence (right) of air.

comonomers segregate at the air side of UV-cured films and PFPAEs are able to dissolve oxygen (Vitale et al., 2013). Thus, it was expected that the fluorinated phase from MMI would migrate toward the air side, causing a surface segregation of the fluorinated domains. The fluorine-enriched phase on the air side then behaves as a protective layer against oxygen inhibition by protecting the reactive maleimide phase from the air. As a result, thanks to the surface segregation, the reaction rate was improved. Moreover, due to the maleimide substituent attached to the fluorinated chain, the fluorinated protective layer is covalently bonded to the network and cannot leach over time.

The photopolymerization kinetics profile of BMI PPO in the presence of the fluorinated additives having more than one functionality in their backbone, BMI C5 and BMI C10, was also studied. In **Figure 3B**, the effect of BMI C10 was examined on the polymerization conversion (similar trends were found for BMI C5). In the absence of air, both BMI C5 and BMI C10 revealed to slow the kinetics of the commercial BMI PPO, even when added in low amount. Nonetheless, the final conversion of the three systems was very similar (**Table 1**). In the presence of air, BMI C10 was also found to act as a protection against oxygen inhibition as discussed before for MMI, by significantly improving the photopolymerization rate of BMI PPO (**Figure 3B**). Similar results would be expected for BMI C5 with a speed increase when added in comparison to the neat BMI PPO product in the presence of air.

Figure 4 compares in details BMI C5 and BMI C10 when added to BMI PPO in different amount and cured in the absence of air. The change in reaction rate and conversion over an irradiation time of 30 s is negligible if the concentration of the fluorinated comonomer is 2 wt%. When the concentration increases to 5 wt%, the conversion showed a slower kinetics for BMI C5; the rate further decreased with BMI C10. Although it has to be noticed that neat BMI C5 and BMI C10 showed differences in their kinetics with faster conversion for BMI C5 than BMI C10 (see supporting information). The difference of kinetics between BMI C5 and BMI C10 could be easily explained by their difference in viscosity: 58 Pa s^{-1} for BMI C10 and 6.6 Pa s^{-1} for BMI C5.

Characterization of the UV-Cured Copolymeric Coatings

The thermal properties of the UV-cured (co)polymers were assessed by TGA and DSC analyses. As reported in **Table 2**, the thermal stability of these polymers was very good thanks to the maleimide group. The temperature corresponding to 5% of weight loss ($T_{5\%}$) for the polymer obtained from the commercial resin BMI PPO was 381°C. In comparison, the fluorinated homopolymers MMI, BMI C5, and BMI C10, respectively had a $T_{5\%}$ of 336, 326, and 325°C. In general, a decrease of the $T_{5\%}$ value was observed when the coatings contained the fluorinated additives, however, its value was always 340°C or higher.

Concerning the glass transition temperature of the systems, the fluorinated homopolymers based on the difunctional BMI C5 and BMI C10 exhibited two T_gs (**Table 2**): the one at low temperatures, around −100°C, corresponded to the fluorinated phase (T_{gF}) and the one above room temperature corresponded to the hydrogenated phase (T_{gH}). The neat MMI polymer showed only one T_g at −66°C. These results suggest that the PFPAE chain present in MMI, characterized by pending $-CF_3$ groups, has a

TABLE 2 | Thermal properties and gel content values of the different mixtures of BMI PPO and the fluorinated additives MMI, BMI C5, and C10.

Sample	BMI PPO (wt%)	PFPAE additive (wt%)	$T_{5\%}$ (°C)	T_{gF}a (°C)	T_{gH}b (°C)
BMI PPO – Neat	100	0	381	n/a	36
BMI PPO + MMI 2%	98	2	379	n/a	40
BMI PPO + MMI 5%	95	5	377	n/a	37
MMI – Neat	0	100	336	−66	n/a
BMI PPO + BMI C5 2%	98	2	379	n/a	61
BMI PPO + BMI C5 5%	95	5	340	n/a	49
BMI C5 – Neat	0	100	326	−100	63
BMI PPO + BMI C10 2%	98	2	357	n/a	62
BMI PPO + BMI C10 5%	95	5	360	n/a	56
BMI C10 – Neat	0	100	325	−105	68

[a]T_g of the fluorinated phase; [b]T_g of the hydrogenated phase.

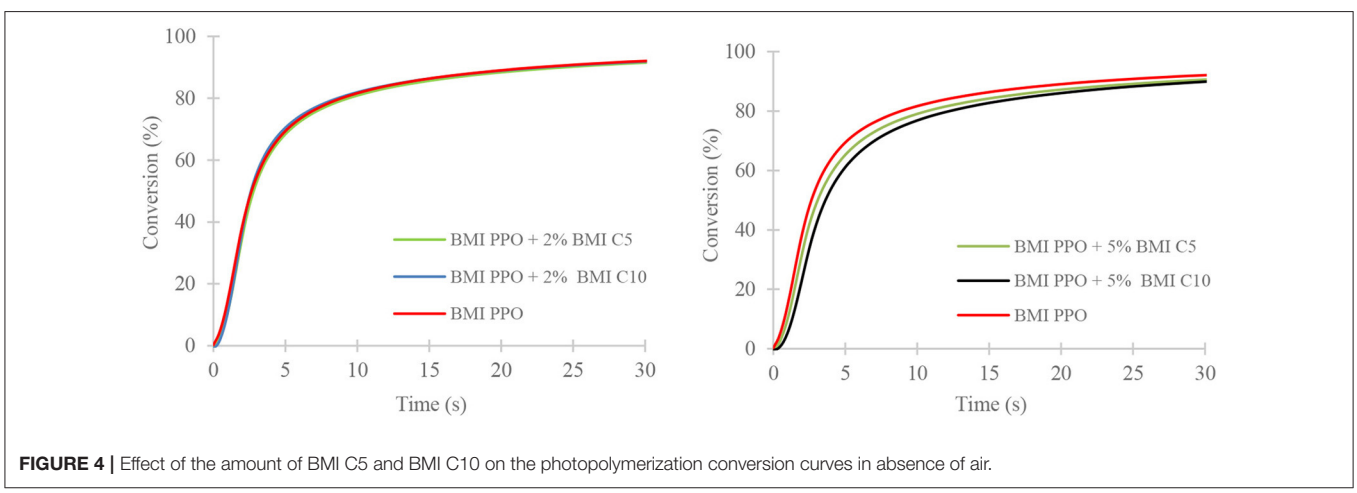

FIGURE 4 | Effect of the amount of BMI C5 and BMI C10 on the photopolymerization conversion curves in absence of air.

restricted mobility, compared to the linear PFPAEs chain present in the BMI monomers.

As shown in **Table 2**, for all the copolymers, only one glass transition temperature (T_{gH}) was detected. T_{gH} was not influenced by the addition of MMI to BMI PPO, even though a slight increase of mobility, due to the pending fluorinated chains bonded only on one side to the polymer network, would be expected. Whereas, T_{gH} was increased by the addition of the less mobile multifunctional additives BMI C5 and BMI C10, which could be due to an enhanced crosslinking of the system.

Contact angle measurements with water and hexadecane (θ_{water} and $\theta_{hexadecane}$, respectively) were performed to determine the surface properties of the coatings (**Table 3**). After detachment from the substrate, measurements were made on the upper side (air side) and on the side in contact with glass (glass side). The commercial BMI PPO polymer showed a water contact angle of around 79° at the air side and a hexadecane contact angle of 21°.

The presence of fluorinated additive had a strong impact on the BMI PPO surface properties. Analyzing the results reported in **Table 3** for the different copolymers, two mains features can be detected. Firstly, the addition of MMI, BMI C5 or BMI C10 increased the contact angle values with water and hexadecane on the air side: values were as high as 109° and 64°, respectively. The fluorinated monomers, although in low amount, imparted omniphobic properties to the coatings on the air side. Secondly, the contact angle values were always higher on the air side than on the glass side, either for water and hexadecane. This phenomenon was assumed to come from the segregation of the fluorinated phase on the air side due to its very poor affinity to glass and its good affinity with air, as reported for other UV-cured systems containing fluorinated comonomers (Vitale et al., 2015). No main difference between the fluorinated additives could be highlighted, as they all led to comparable contact angle values.

XPS analyses (**Table 4**) confirmed the segregation of the fluorinated monomers at the air surface as commonly found in literature (Casazza et al., 2002; Hu et al., 2008; Bongiovanni et al., 2012). Indeed, the percentage of fluorine was found to be much higher on the air side than on the glass side for the copolymeric coatings. Moreover, while the percentages of the fluorinated additives were low, i.e., around 0.01 mol% for the copolymers containing 5 wt% of comonomer, at the air surface the amount of fluorine greatly exceeded the calculated values (**Table 4**). As an example, the sample containing MMI has a 100-fold increase of the atomic percentage of fluorine at the air surface. The values of the fluorine atomic percentage of the pure fluorinated comonomers, calculated on the basis of their chemical structure (**Figure 1**), are 51, 35, and 31% for MMI, BMI C5 and BMI C10, respectively. Therefore, it is demonstrated that at the air surface there is a fluorinated layer, which contains nearly exclusively the PFPAE comonomer. These results clearly explain the high contact angle values with water and hexadecane on the air side and the protection from oxygen inhibition.

TABLE 3 | Contact angles of the different copolymers of BMI PPO and fluorinated additives.

Sample	BMI PPO (wt%)	PFPAE additive (wt%)	θ_{water} (°)		$\theta_{hexadecane}$ (°)	
			Air side	Glass side	Air side	Glass side
BMI PPO – Neat	100	0	79 ± 2	83 ± 3	21 ± 1	32 ± 1
BMI PPO + MMI 2%	98	2	109 ± 1	76 ± 2	64 ± 1	40 ± 3
BMI PPO + MMI 5%	95	5	98 ± 1	63 ± 2	62 ± 0	46 ± 0
MMI – Neat	0	100	124 ± 3	n/a	82 ± 3	n/a
BMI PPO + BMI C5 2%	98	2	101 ± 2	73 ± 3	62 ± 1	46 ± 1
BMI PPO + BMI C5 5%	95	5	102 ± 1	69 ± 2	63 ± 0	42 ± 3
BMI C5 – Neat	0	100	108 ± 1	104 ± 1	68 ± 3	55 ± 1
BMI PPO + BMI C10 2%	98	2	101 ± 1	62 ± 2	64 ± 0	41 ± 3
BMI PPO + BMI C10 5%	95	5	99 ± 2	64 ± 1	62 ± 1	46 ± 3
BMI C10 – Neat	0	100	110 ± 1	103 ± 1	71 ± 2	72 ± 1

CONCLUSIONS

Different fluorinated PFPAE-based maleimides were synthesized with different degree of functionality. They were employed at a low content as a comonomer in the photopolymerization of bismaleimide poly(propylene oxide) resin (BMI PPO). The fluorinated maleimides displayed an interesting behavior under

TABLE 4 | XPS measurements of the different copolymers of BMI PPO and fluorinated additives: atomic percentage composition of the coatings surfaces.

Sample	BMI PPO (wt%)	PFPAE additive (wt%)	Air side				Glass side			
			C_{1s}	O_{1s}	F_{1S}	N_{1s}	C_{1s}	O_{1s}	F_{1S}	N_{1s}
BMI PPO – Neat	100	0	69.9	25.2	/	4.9	71.3	23.6	/	5.1
BMI PPO + MMI 5% experimental values	95	5	44.3	13.2	40.9	1.7	70.1	23.4	1.5	5.0
Calculated values			68.7	24.1	0.49	6.9				
BMI PPO + BMI C5 5% experimental values	95	5	44.4	20.6	32.7	2.3	60.7	23.5	11.7	4.1
Calculated values			68.9	24.1	0.34	6.8				
BMI PPO + BMI C10 5% experimental values	95	5	57.6	23.7	15.0	3.7	68.5	24.5	1.9	5.1
Calculated values			68.8	24.1	0.26	6.8				

UV-light: in the presence of air they acted as a protective layer against oxygen inhibition, allowing an increase of the photopolymerization rate. The final coatings exhibited a good thermal stability due to the maleimide structure as well as an omniphobic behavior. Indeed, the surface properties of BMI PPO were modified thanks to the surface segregation of the fluorinated additives. These results are very encouraging in view of industrial application to overcome the oxygen inhibition effect and at the same time tune the surface properties of coatings.

DATA AVAILABILITY STATEMENT

The datasets generated for this study are available on request to the corresponding author.

AUTHOR CONTRIBUTIONS

JB was involved in the synthesis of the monomers. CB participated to the synthesis and investigated the photopolymerization of the new monomers as well as their characterization. GT and AV also did the characterization of the polymers. CJ-D led the conception of the work. CF and RB supervised the work as part of a H2020 project, contributed to the data analysis and interpretation. RB and CB prepared the manuscript. All authors contributed to its revision, read, and approved the submitted version.

FUNDING

This research project has received funding from the European Union's Horizon 2020 research and innovation program under grant agreement No. 690917—PhotoFluo; Natural Sciences and Engineering Research Council of Canada (NSERC), Discovery Grants Program RGPIN-2015-05513 and Ministère de l'Enseignement Supérieure et de la Recherche. We would also like to thank Valérie Flaud and Jérôme Esvan for their efforts concerning the XPS analyses.

REFERENCES

Ameduri, B., and Boutevin, B. (eds.). (2004). "Chapter 3: Synthesis, properties and applications of fluoroalternated copolymers," in *Well-Architectured Fluoropolymers: Synthesis, Properties and Applications* (Amsterdam: Elsevier), 187–230. doi: 10.1016/B978-008044388-1/50012-1

Bongiovanni, R., Medici, A., Zompatori, A., Garavaglia, S., and Tonelli, C. (2012). Perfluoropolyether polymers by UV curing: design, synthesis and characterization. *Polym. Int.* 61, 65–73. doi: 10.1002/pi.3149

Bonneaud, C., Burgess, J. M., Bongiovanni, R., Joly-Duhamel, and, C., and Friesen, C. M. (2019). Photopolymerization of maleimide perfluoropolyalkylethers without a photoinitiator. *J. Polym. Sci. A Pol. Chem.* 57, 699–707. doi: 10.1002/pola.29311

Bowman, C. N., and Kloxin, C. J. (2008). Toward an enhanced understanding and implementation of photopolymerization reactions. *AIChE J.* 54, 2775–2795. doi: 10.1002/aic.11678

Casazza, E., Ricco, L., Russo, S., and Mariani, A. (2002). Synthesis, characterization, and properties of a novel acrylic terpolymer with pendant perfluoropolyether segments. *Polymer* 43, 1207–1214. doi: 10.1016/S0032-3861(01)00722-4

Corrigan, N., Yeow, J., Judzewitsch, P., Xu, J., and Boyer, C. (2019). Seeing the light: advancing materials chemistry through photopolymerization. *Angew. Chem. Int. Ed.* 58, 5170–5189. doi: 10.1002/anie.201805473

Crivello, J. V., and Reichmanis, E. (2014). Photopolymer materials and processes for advanced technologies. *Chem. Mater.* 26, 533–548. doi: 10.1021/cm402262g

Decker, C., Bianchi, C., and Jönsson, S. (2004). Light-induced crosslinking polymerization of a novel N-substituted bis-maleimide monomer. *Polymer*. 45, 5803–5811. doi: 10.1016/j.polymer.2004.06.047

Du, Y., Williams, B. A., Francis, L. F., and McCormick, A. V. (2017a). Pulsed irradiation for high-throughput curing applications. *Prog. Org. Coat.* 104, 104–109. doi: 10.1016/j.porgcoat.2016.12.012

Du, Y., Xu, J., Sakizadeh, J. D., Weiblen, D. G., McCormick, A. V., and Francis, L. F. (2017b). Modulus- and surface-energy-tunable thiol–ene for UV micromolding of coatings. *ACS Appl. Mater. Interfaces* 9, 24976–24986. doi: 10.1021/acsami.7b06339

Friesen, C. M., and Ameduri, B. (2018). Outstanding telechelic perfluoropolyalkylethers and applications therefrom. *Prog. Polym. Sci.* 81, 238–280. doi: 10.1016/j.progpolymsci.2018.01.005

Hoyle, C. E., and Bowman, C. N. (2010). Thiol-ene click chemistry. *Angew. Chem. Int. Ed.* 49, 1540–1573. doi: 10.1002/anie.200903924

Hoyle, C. E., Clark, S. C., Jonsson, S., and Shimose, M. (1997). Photopolymerization using maleimides as photoinitiators. *Polymer* 38, 5695–5697. doi: 10.1016/S0032-3861(97)00181-X

Hu, Z., Chen, L., Betts, D. E., Pandya, A., Hillmyer, M. A., and DeSimone, J. M. (2008). Optically transparent, amphiphilic networks based on blends of perfluoropolyethers and poly(ethylene glycol). *J. Am. Chem. Soc.* 130, 14244–14252. doi: 10.1021/ja803991n

Jönsson, S., Sundell, P. E., Shimose, M., Clark, S., Miller, C., Morel, F., et al. (1997). Photo-induced alternating copolymerization of N-substituted maleimides and electron donor olefins. *Nucl. Instrum. Nucl. Instrum. Methods Phys. Res. B* 131, 276–290. doi: 10.1016/S0168-583X(97)00136-5

Ligon, S. C., Husár, B., Wutzel, H., Holman, R., and Liska, R. (2014). Strategies to reduce oxygen inhibition in photoinduced polymerization. *Chem. Rev.* 114, 557–589. doi: 10.1021/cr3005197

Ligon, S. C., Liska, R., Stampfl, J., Gurr, M., and Mülhaupt, R. (2017). Polymers for 3D printing and customized additive manufacturing. *Chem. Rev.* 117, 10212–10290. doi: 10.1021/acs.chemrev.7b00074

Malinverno, G., Pantini, G., and Bootman, J. (1996). Safety evaluation of perfluoropolyethers, liquid polymers used in barrier creams and other skin-care products. *Food Chem. Toxicol.* 34, 639–650. doi: 10.1016/0278-6915(96)00023-3

Pantini, G. (2008). Perfluoropolyether phosphate: a non-irritating acidic agent of cosmeceutical use. *Clin. Dermatol.* 26, 387–391. doi: 10.1016/j.clindermatol.2008.04.005

Pozos vázquez, C., Tayouo, R., Joly-Duhamel, C., and Boutevin, B. (2010). UV-curable bismaleimides containing poly(dimethylsiloxane): use as hydrophobic agent. *J. Polym. Sci. A Pol. Chem.* 48, 2123–2134. doi: 10.1002/pola.23980

Soules, A., Pozos Vázquez, C., Ameduri, B., Joly-Duhamel, C., Essahli, M., and Boutevin, B. (2008). Use of fluorinated maleimide and telechelic bismaleimide for original hydrophobic and oleophobic polymerized networks. *J. Polym. Sci. A Pol. Chem.* 46, 3214–3228. doi: 10.1002/pola.22658

Vázquez, C. P., Joly-Duhamel, C., and Boutevin, B. (2009). Photopolymerization without photoinitiator of bismaleimide-containing oligo(oxypropylene)s: effect of oligoethers chain length. *Macromol. Chem. Phys.* 210, 269–278. doi: 10.1002/macp.200800510

Vitale, A., Bongiovanni, R., and Ameduri, B. (2015). Fluorinated oligomers and polymers in photopolymerization. *Chem. Rev.* 115, 8835–8866. doi: 10.1021/acs.chemrev.5b00120

Vitale, A., Priola, A., Tonelli, C., and Bongiovanni, R. (2013). Nanoheterogeneous networks by photopolymerization of perfluoropolyethers and acrylic co-monomers. *Polym. Int.* 62, 1395–1401. doi: 10.1002/pi.4436

Vitale, A., Touzeau, S., Sun, F., and Bongiovanni, R. (2018). Compositional gradients in siloxane copolymers by photocontrolled surface segregation. *Macromolecules* 51, 4023–4031. doi: 10.1021/acs.macromol.8b00339

von Sonntag, J., Beckert, D., Knolle, W., and Mehnert, R. (1999). Electron transfer as the initiation mechanism of photocurable maleimide–vinyl ether based resins. *Radiat. Phys. Chem.* 55, 609–613. doi: 10.1016/S0969-806X(99)00256-X

von Sonntag, J., and Knolle, W. (2000). Maleimides as electron-transfer photoinitiators: quantum yields of triplet states and radical-ion formation. *J. Photochem. Photobiol. A Chem.* 136, 133–139. doi: 10.1016/S1010-6030(00)00313-0

Wang, Z., Cousins, I. T., Scheringer, M., and Hungerbuehler, K. (2015). Hazard assessment of fluorinated alternatives to long-chain perfluoroalkyl acids (PFAAs) and their precursors: status quo, ongoing challenges and possible solutions. *Environ. Int.* 75, 172–179. doi: 10.1016/j.envint.2014.11.013

Wasser, L., Dalle Vacche, S., Karasu, F., Müller, L., Castellino, M., Vitale, A., et al. (2018). Bio-inspired fluorine-free self-cleaning polymer coatings. *Coatings* 8:436. doi: 10.3390/coatings8120436

Yagci, Y., Jockusch, S., and Turro, N. J. (2010). Photoinitiated polymerization: advances, challenges, and opportunities. *Macromolecules* 43, 6245–6260. doi: 10.1021/ma1007545

Yamada, M., Takase, I., and Koutou, N. (1968). Photopolymerization of maleimide and its N-substituted derivatives. *J. Polym. Sci. B Polym. Let.* 6, 883–888. doi: 10.1002/pol.1968.110061211

Zhang, C., Moonshi, S. S., Wang, W., Ta, H. T., Han, Y., Han, F. Y., et al. (2018). High F-content perfluoropolyether-based nanoparticles for targeted detection of breast cancer by 19 F magnetic resonance and optical imaging. *ACS Nano*. 12, 9162–9176. doi: 10.1021/acsnano.8b03726

Conflict of Interest: The authors declare that the research was conducted in the absence of any commercial or financial relationships that could be construed as a potential conflict of interest.